

## Imaging Evaluation after Stereotactic Body Radiotherapy for Hepatocellular Carcinoma: Prognostic Value of Radiological Changes

KY Man,<sup>1</sup> YS Luk,<sup>1</sup> ALY Law,<sup>2</sup> WKW Leung<sup>1</sup>

<sup>1</sup>Department of Radiology, Pamela Youde Nethersole Eastern Hospital, Chai Wan, Hong Kong

<sup>2</sup>Department of Clinical Oncology, Pamela Youde Nethersole Eastern Hospital, Chai Wan, Hong Kong

### ABSTRACT

**Objective:** To evaluate the computed tomography and magnetic resonance imaging features of tumour response and predictive factors of time to progression and survival after stereotactic body radiotherapy for hepatocellular carcinoma.

**Methods:** Consecutive patients with hepatocellular carcinoma who were treated by stereotactic body radiotherapy between June 2006 and September 2016 were included in this retrospective study. Clinical and radiological data obtained using computed tomography or magnetic resonance imaging were examined. The response rate, in-field local control, time to progression, overall survival and prognostic factors were evaluated. Treatment response was classified according to modified Response Evaluation Criteria in Solid Tumors.

**Results:** In total, 73 patients were included. The complete response, partial response, stable disease, and disease progression rates were 41.1%, 20.5%, 27.4% and 11% respectively. The in-field local control rates at 1 year and 2 years were 95.9% and 92.1%, respectively. The median follow-up time was 19 months and the median overall survival was 20 months. T1-weighted or T2-weighted signal intensities, pattern of lipiodol stain, complete thin rim enhancement and focal liver reaction in post-treatment images were shown to be independent predictors for progression or overall survival.

**Conclusion:** Imaging evaluation of tumour response is important. Recognising and interpreting the radiological features of tumour response (both tumour and juxtaposed non-tumourous hepatic parenchyma) is essential in making an accurate assessment of treatment response. Accurate imaging evaluation may also help predict survival.

**Key Words:** Carcinoma, hepatocellular; Magnetic resonance imaging; Radiosurgery; Tomography, X-ray computed

---

**Correspondence:** Dr KY Man, Department of Radiology, Pamela Youde Nethersole Eastern Hospital, Chai Wan, Hong Kong.  
Email: [dsgundam@hotmail.com](mailto:dsgundam@hotmail.com)

Submitted: 14 May 2018; Accepted: 26 Jun 2018.

Contributors: KYM was responsible for the design of study, acquisition and analysis of data, and wrote the article. All authors (KYM, YSL, ALYL, and WKWL) made critical revisions of the intellectual content of this article. All authors had full access to the data, contributed to the study, approved the final version for publication, and take responsibility for its accuracy and integrity.

Conflicts of Interest: All authors have disclosed no conflicts of interest.

Funding/Support: This research received no specific grant from any funding agency in the public, commercial, or not-for-profit sectors.

Ethics Approval: This study was approved by the Hong Kong East Cluster Research Ethics Committee (Ref HKECREC-2017-083). Informed consent was obtained by patients for all procedures.

## 中文摘要

### 肝細胞癌體部立體定向放療：影像預後分析

文家潤、陸嬌、羅麗柔、梁錦榮

**目的：**分析接受體部立體定向放療（SBRT）的肝細胞癌（HCC）患者的電腦斷層掃描和磁力共振掃描影像。評估腫瘤反應和其對總生存率的預後關係。

**方法：**回顧2006年6月至2016年9月期間接受SBRT治療的HCC患者的電腦斷層掃描和磁力共振掃描影像。評估腫瘤反應、野內局部控制率、疾病惡化時間、總生存率和預後因素。根據修改版實體腫瘤療效評估標準（RECIST）對治療反應進行分類。

**結果：**共納入73名患者。完全緩解、部分緩解、疾病穩定和疾病進展率分別為41.1%、20.5%、27.4%和11%。1年和2年野內局部控制率分別為95.9%和92.1%。中位隨訪19個月後，中位生存期為20個月。治療後影像的T1W/T2W信號轉變、lipiodol腫瘤染色現象、週邊邊緣密度增強以及局部肝反應均能獨立預測疾病惡化時間或總生存率。

**結論：**透過影像分析腫瘤反應是相當重要。識別和詮釋腫瘤反應的放射學特徵（腫瘤和並列的非腫瘤性肝實質）對於準確評估治療反應至關重要。精確分析影像能幫助預測總生存率。

## INTRODUCTION

Hepatocellular carcinoma (HCC) is the fifth most common malignant neoplasm and the third most common cause of cancer-related death worldwide.<sup>1</sup> Liver cancer is the fourth most common cancer type and third most common cause of cancer deaths in Hong Kong. The crude incidence rate and mortality rate for liver cancer are 25.5 and 21.9 per 100000 population, respectively.<sup>2</sup> Liver malignancy, in particular HCC, continues to be a major health concern.

For inoperable tumours, the treatment options are limited. For example, transarterial chemoembolisation (TACE), systemic therapy, and best supportive care are generally reserved for inoperable tumours.<sup>3</sup> Stereotactic body radiotherapy (SBRT), or stereotactic ablative radiotherapy, has recently been identified as an alternative or complementary treatment for patients with HCC. Several studies have reported the safety of SBRT, as well as high rates of local control.<sup>4-7</sup> SBRT is a noninvasive method of treatment for primary hepatic tumours. Ablative doses of radiation are delivered to a target volume in a single or small number of high-dose fractions. SBRT is performed with a steep dose gradient and rapid dose fall-off outside of the target, to minimise the dose to adjacent normal tissues.

Imaging evaluation of tumour response is important. Learning how to recognise and interpret radiological features is essential in making an accurate assessment

of treatment response and in guiding subsequent management. Many studies have described assessment of HCC response to locoregional treatment and clinical prognostic factors for SBRT to HCC.<sup>8-17</sup> Common response assessment criteria include the guidelines of the World Health Organization,<sup>18</sup> Response Evaluation Criteria in Solid Tumors (RECIST),<sup>19</sup> and the European Association for the Study of the Liver,<sup>20</sup> and the modified RECIST (mRECIST).<sup>21</sup> However, there is limited information on examining other image parameters for predicting the treatment outcome of HCC treated with SBRT.

This study aimed to evaluate the computed tomography (CT) and magnetic resonance imaging (MRI) features of tumour response for HCC treated with SBRT and to identify specific imaging characteristics (both tumour and juxtaposed non-tumourous hepatic parenchyma) as prognostic factors.

## METHODS

### Patients

This retrospective study included consecutive patients who underwent high-dose conformal radiotherapy for HCC between June 2006 and September 2016 in Pamela Youde Nethersole Eastern Hospital, Hong Kong. The diagnosis of HCC could be made on radiological or pathological basis.<sup>20</sup> For each patient with HCC, the treatment strategy was discussed by a multidisciplinary team that included hepatologists, hepatobiliary surgeons, radiation oncologists, and radiologists. The inclusion

criteria for high-dose conformal radiotherapy for HCC were (1) Primary HCC (radiological or histological confirmation); (2) liver confined disease; (3) unresectable, medically inoperable tumour or patient's refusal; (4) serum bilirubin <3 times upper range of normal, ALT <5 times upper range of normal and creatinine <150  $\mu\text{mol/L}$ . Exclusion criteria were (1) clinical ascites; (2) hepatic encephalopathy; (3) presence of distant metastasis. All patients provided written informed consent to receive SBRT. The clinical data were obtained through dedicated electronic patient record system and patient demographics were recorded. All data of patient records were anonymised and de-identified prior to analysis.

### Treatment with Stereotactic Body Radiotherapy

All patients were immobilised in a supine position with their arms over their heads. SBRT was delivered with respiratory-control and image guidance. A real-time position management system (Varian Trilog<sup>TM</sup>; Varian Medical Systems, Palo Alto [CA], US) was used for passive real-time monitoring of patient respiration for the purpose of intra-fraction motion management. Using simulator fluoroscopy, the breathing trace was registered to the motion of the tumour site. The tumours were treated under breath-hold at end-expiration, or with free breathing only if the patient did not comply with the breath-hold requirements. An on-board imager (Varian Trilog; Varian Medical Systems) providing high quality kV images was used in every fraction for accurate and precise patient positioning before delivery of SBRT.

For patients treated before March 2014, gross tumour volume was outlined on the planning CT images; taking into consideration all the prior images including tri-phasic contrast-enhanced CT scan, lipiodol CT scan, ultrasound imaging, and angiogram. The clinical target volume included the gross tumour volume with an 8-mm margin. The clinical target volume was then expanded asymmetrically, 5 mm in the lateral and 8 mm in the craniocaudal direction for setup uncertainty, to produce the planning target volume (PTV). Three-dimensional conformal treatment plans were produced with 6-MV X-ray scans. The prescribed dose to the PTV was 55 Gy over 10 fractions (equivalent to 71 Gy equivalent dose in 2-Gy fractions [EQD2] using an  $\alpha/\beta$  ratio of 10 Gy). The mean dose to the normal liver was kept below 22 Gy. The allowed maximum dose to the spinal cord was 34 Gy. No more than 33% combined kidney volume should receive 18 Gy or more. No more than 1 cc of bowel, 1 cc of duodenum and 1 cc of stomach were allowed to

receive more than 37 Gy. Lower prescribed doses were used on some patients in order to satisfy the normal tissue complication probability constraints.<sup>22</sup>

Since March 2014, a new hypofractionation protocol has been applied. With this protocol the clinical target volume was identical to the gross tumour volume, which was then expanded asymmetrically as described above to produce the PTV. The prescribed dose to the PTV was 50 Gy over 5 daily fractions (EQD2 = 83.3 Gy). The dose constraint followed the Radiation Therapy Oncology Group 1112 protocol.<sup>23</sup> In this study both treatment schemes are described as SBRT for simplicity.

### Computed Tomography and Magnetic Resonance Imaging Technique and Analysis

Regular contrast CT imaging was performed after radiotherapy (at 3-month intervals in the first year after SBRT and less frequently in subsequent years) for follow-up assessment. CT scans were obtained with 64 multidetector CT scanners (SOMATOM Definition AS+ 64-slice CT scanner; Siemens AG, Erlangen, Germany or Aquilion CX 64-slice CT scanner; Toshiba Medical Systems Corporation, Otawara, Japan) in the unenhanced, arterial, portovenous and delayed phases. Patients were given 80 to 90 mL of Iohexol (Omnipaque 350; GE Healthcare, Chicago [IL], US) at 2.3 to 2.5 mL/s via an 18-to-20-G intravenous cannula. Arterial phase images were obtained using a bolus tracking technique with a trigger enhancement threshold at the upper abdominal aorta of 120 HU (SOMATOM; Siemens) or 180 HU (Aquilion; Toshiba). Portovenous phase images were obtained with a delay of 60 s after the arterial phase acquisition. Delay phase images were obtained at 5 minutes after contrast injection.

The MRI examinations were performed on a 1.5-T scanner (MAGNETOM Avanto 1.5T; Siemens). Typical MRI protocol in our institution is summarised in Table 1. Contrast MRI abdomen was performed when CT findings were equivocal.

The CT and MR images were retrospectively reviewed and quantitative and qualitative CT and MRI radiological features were recorded. Each image set was reviewed in randomised order by two independent radiologists with 5 and 10 years of abdominal radiology experience, who were blinded to the clinical, laboratory, and pathologic information. The radiologists independently determined the after CT and MRI quantitative and qualitative imaging features (including pre- and post-treatment images): (a)

**Table 1.** Typical protocol for liver MRI with extracellular fluid contrast agent (gadoterate meglumine) in our institution.

Protocol step	
Pre-contrast imaging	CoronalTruff <sup>1</sup> Axial T1-weighted in- and opposed-phase GRE <sup>2</sup> Axial T1-weighted VIBE FS <sup>3</sup> T2-weighted FS fast SE non-breath hold <sup>4</sup>
Contrast agent injection	0.01-mmol/kg intravenous bolus (2 mL/s)
Dynamic imaging <sup>5</sup>	Axial T1-weighted VIBE FS Diffusion-weighted imaging / apparent diffusion coefficient <sup>6</sup>

Abbreviations: 2D = two-dimensional; 3D = three-dimensional; FS = fat-suppressed; GRE = gradient echo; SE = spin echo; VIBE = volumetric interpolated breath-hold examination.

1: True fast imaging with steady-state free precession (3.3/1.4 [repetition time ms/echo time ms]; flip angle 60°; section thickness 6 mm).

2: 227/2.4 (repetition time ms/echo time ms); second TE 4.87 ms; flip angle 70°; section thickness 7 mm.

3: VIBE sequence. Spoiled 3D GRE sequence (4.7/2.4 [repetition time ms/echo time ms]; flip angle 10°, section thickness 3 mm).

4: 3635/72 (repetition time ms/echo time ms); flip angle 150°, section thickness 3 mm.

5: Performed at 30, 90, and 300 s after the start of contrast agent injection (hepatic arterial, portovenous, and delay phases).

6: Diffusion-weighted imaging, apparent diffusion coefficient 8729/83 (repetition time ms/echo time ms); section thickness 7 mm; b value 50/300/600).

longest diameter of the target viable HCC, which should be performed on CT or MRI obtained in the arterial phase when the contrast between viable vascularised tumour tissue and non-enhancing necrotic tissue is the highest<sup>21</sup>; (b) whether there was solitary or multiple HCCs in pre-treatment images<sup>16</sup>; (c) macroscopic portal vein invasion, defined as invasion of the adjacent portal veins grossly visible on images<sup>16</sup>; (d) location of tumour, ie, whether the tumour was in right or left lobe, and whether the lesion border was within 1 cm of the liver dome<sup>12</sup> or liver capsule<sup>16</sup>; (e) lipiodol distribution (if any) within a lesion (whether there was minimal, partial or diffuse distribution)<sup>12</sup>; (f) T1- weighted or T2-weighted signal intensities of target lesion in post-treatment MRI<sup>8</sup>; (g) whether there was complete thin rim enhancement of target lesion in post-treatment CT or MRI<sup>8,17</sup>; and (h) presence of focal liver reaction or delay phase hyperenhancement over irradiated juxtaposed non-tumourous hepatic parenchyma in CT or MRI images in 6-month intervals.<sup>17,24</sup> If there was a discrepancy between the reviewers, the final evaluation result was reached by consensus decision.

### Tumour Response, Tumour Local Control, Time to Progression, and Overall Survival

Treatment response was evaluated according to

mRECIST.<sup>21</sup> A complete response was defined as the disappearance of any intratumoural arterial enhancement in target lesions. A 30% decrease or more in the sum of diameters of viable (enhancement in the arterial phase) target lesions, taking as reference the baseline sum of the diameters of target lesions, was judged to be a partial response. An increase of at least 20% in the sum of the diameters of viable (enhancing) target lesions, taking as reference the smallest sum of the diameters of viable (enhancing) target lesions recorded since treatment started, was judged to be disease progression. Any cases that did not qualify for either partial response or disease progression were judged to be stable disease. In-field local control was defined as the absence of disease progression within the PTV on follow-up imaging or pathological analysis.<sup>15</sup> Time to progression was calculated from day of last SBRT treatment session. Progression was defined as having either (a) disease progression within PTV; (b) new liver lesions outside PTV (out of field failure); or (c) extrahepatic metastasis. Overall survival was calculated as the time from the last fraction of SBRT until death from any cause. Patients were censored on the day of last imaging for all local control and time to progression analyses. Overall survival with censoring to last follow-up examination or liver transplantation was assessed.<sup>15,24</sup> The incidence of radiation-induced liver disease, which includes anicteric ascites with an elevation of alkaline phosphatase in relation to the liver transaminases, was also analysed. Radiation-induced liver disease may occur within 3 months after SBRT and has always been a limiting factor for radiotherapy as it can result in liver failure and death.<sup>25</sup>

### Statistical Analysis

All analyses were undertaken using SPSS (Windows version 22; IBM Corp., Armonk [NY], US). Sample size was based on published literature and pilot data (portal vein thrombosis hazard ratio (HR) = 2.54; median survival for patient without portal vein thrombosis = 14 months<sup>15</sup>; planned average length of follow-up time = 12 months; other radiological features used in this study being exploratory in nature). By using a two-tailed  $\alpha$  value of 0.05, a sample size of 33 patients per group would result in 80% power to detect this effect size. 10% was added to account for patient attrition, leading to an overall sample size of 73 patients. Time to progression and overall survival were estimated using Kaplan-Meier method, and the differences were evaluated using log-rank test. The univariate Cox proportional-hazards regression model was used to determine the imaging predictors of liver cancer, time to progression, and overall survival.

Factors with a *p* value of <0.05 were then included in the multivariable proportional-hazards regression model. The MRI features variables would be excluded from the multivariable model due to limited sample size. A forward stepwise regression model was used. Differences were considered statistically significant if *p* < 0.05.

## RESULTS

### Patients, Treatment, and Radiological Characteristics

In total, 73 consecutive patients who underwent high-dose conformal radiotherapy were included. Median age of the patients was 70 years (range, 48-88 years). Most patients had hepatitis B cirrhosis (75.3%), Child-Pugh

class A cirrhosis (78.1%), Barcelona Clinic Liver Cancer classification stage C disease (86.3%), and Eastern Cooperative Oncology Group performance status 1 (76.7%). Nearly half of the patients received TACE before the SBRT treatment (46.6%). Four patients had liver transplantation after SBRT; 26 had at least one progress MRI after SBRT. Patient characteristics are detailed in Table 2.

In total, 57 patients (78%) received 50-55 Gy in 10 fractions and 16 (22%) received 45 to 50 Gy in 5 fractions. Median follow-up time was 19 months. Median maximal target HCC diameter was 3 cm. Patient radiological features are detailed in Table 3.

**Table 2.** Characteristics of patients and treatment.\*

Characteristics	Value
Age (years)	70 (18; 48-88)
Sex	
Male	54 (74%)
Female	19 (26%)
Follow-up time (months)	19 (28; 5-120)
Aetiology of cirrhosis	
Hepatitis B virus	55 (75.3%)
Hepatitis C virus	7 (9.6%)
Alcoholism	4 (5.5%)
Other	7 (9.6%)
BCLC Stage	
Early stage (A)	4 (5.5%)
Intermediate stage (B)	1 (1.4%)
Advanced stage (C)	63 (86.3%)
Terminal stage (D)	5 (6.8%)
Child-Pugh class	
A	57 (78.1%)
B	14 (19.2%)
C	2 (2.7%)
Performance status	
0	5 (6.8%)
1	56 (76.7%)
2	8 (11.0%)
3	4 (5.5%)
Previous treatment for HCC	
None	9 (12.3%)
TACE alone	34 (46.6%)
RFA alone	5 (6.8%)
Surgery alone	1 (1.4%)
Combination of therapies	24 (32.9%)
Liver transplantation	
No	69 (94.5%)
Yes	4 (5.5%)
At least one progress MRI after SBRT	
No	47 (64.4%)
Yes	26 (35.6%)
Total dose/No. of fractions	
50-55 Gy/10 fr	57 (78.1%)
45-50 Gy/6 fr	16 (21.9%)

Abbreviations: BCLC = Barcelona Clinic Liver Cancer Staging Classification; RFA = radiofrequency ablation; SBRT = stereotactic body radiotherapy; TACE = transarterial chemoembolisation.

\* Data are shown as No. (%) or median (interquartile range; range).

**Table 3.** Characteristics of radiological features.\*

Characteristics	Value
Maximum target tumour diameter (cm)	3 (2.2; 1.1-17)
≤3 cm	42 (57.5%)
>3 cm	31 (42.5%)
Multiple lesions at baseline	
Single lesion	39 (53.4%)
Multiple lesions	34 (46.6%)
Macroscopic portal vein thrombosis	
No	63 (86.3%)
Yes	10 (13.7%)
Location near liver dome	
>1 cm away from dome	49 (67.1%)
≤1 cm away from dome	24 (32.9%)
Location near liver capsule	
>1 cm away from capsule	19 (26.0%)
≤1 cm away from capsule	54 (74.0%)
Location of tumour	
Right lobe	58 (79.5%)
Left lobe	15 (20.5%)
Pattern of lipiodol stain (if any (n = 48))	
Minimal	4 (8.3%)
Partial or heterogeneous	28 (58.3%)
Diffuse or homogeneous	16 (33.3%)
Presence of focal liver reaction in post-treatment computed tomography	
No	20 (27.4%)
Yes	53 (72.6%)
Presence of focal liver reaction in post-treatment magnetic resonance imaging (n = 24)	
No	6 (25.0%)
Yes	18 (75.0%)
T1-weighted signal intensity in post-treatment magnetic resonance imaging (n = 26)	
Hypointense	4 (15.4%)
Hyperintense	22 (84.6%)
T2-weighted signal intensity in post-treatment magnetic resonance imaging (n = 26)	
Hypointense	23 (88.5%)
Hyperintense	3 (11.5%)
Complete thin rim enhancement in post-treatment images (n = 67)	
No	43 (64.2%)
Yes	24 (35.8%)

\* Data are shown as No. (%) or median (interquartile range; range).

### Primary and Secondary Outcomes

No radiation-induced liver disease was observed in our study cohort. 30 patients (41.1%) had decompensated cirrhosis or liver failure more than 3 months after SBRT, probably due to natural progression of cirrhosis not related to SBRT. Two of the treated patients (2.7%) died of gastrointestinal bleeding after treatment. For these two patients, the PTVs were not in the proximity of the stomach or small bowels; they both had oesophageal varices as confirmed by upper gastrointestinal endoscopy. Eight patients died of chest infection.

**Table 4.** Primary and secondary outcomes.\*

Characteristics	Value
Tumour response as per mRECIST	
Complete response	30 (41.1%)
Partial response	15 (20.5%)
Stable disease	20 (27.4%)
Disease progression	8 (11.0%)
1-year local control	
No	3 (4.1%)
Yes	70 (95.9%)
2-year local control	
No	3 (7.9%)
Yes	35 (92.1%)
Time to progression (months)	14 (12-16)
Overall survival (months)	20 (15-25)

Abbreviation: mRECIST = modified Response Evaluation Criteria in Solid Tumors.

\* Data are shown as No. (%) or median (95% confidence interval).

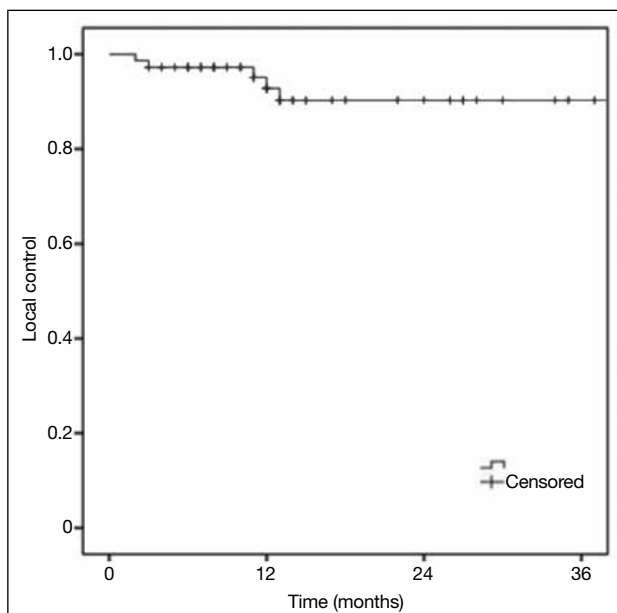


**Figure 1.** Kaplan-Meier curve for local control. The 1-year local control and 2-year local control rates were 95.9% and 92.1% respectively.

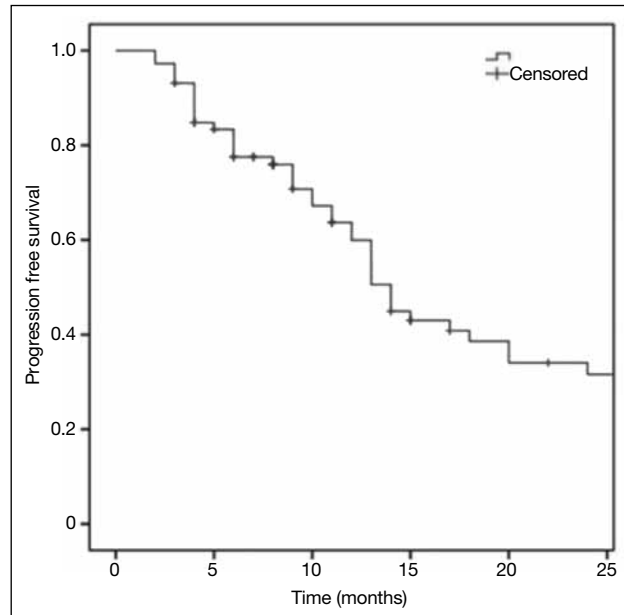


**Figure 2.** Kaplan-Meier curve for progression-free survival. The median time to progression was 14 months.

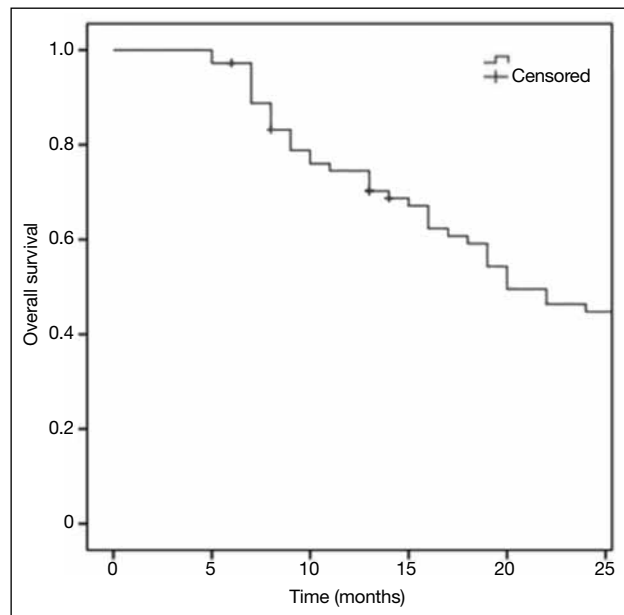


**Figure 3.** Kaplan-Meier curve for overall survival. The median overall survival was 20 months.

Primary and secondary outcomes are detailed in Table 4 and Figures 1 to 3. The tumour complete response, partial response, stable disease, and disease progression rates were 41.1%, 20.5%, 27.4% and 11% respectively. The in-field local control rates at 1 year and 2 years were 95.9% and 92.1%, respectively. Median time to progression was 14 months. The median overall survival

**Table 5.** Univariate Cox regression analyses of radiological predictive factors for primary and secondary outcomes.\*

Radiological features	Local control		Time to progression		Overall survival	
	HR (95% CI)	p Value	HR (95% CI)	p Value	HR (95% CI)	p Value
Maximum target tumour diameter (cm)						
≤3 cm	1		1		1	
>3 cm	1.2 (0.28-4.9)	0.828	1.16 (0.87-1.56)	0.316	1.15 (0.68-1.94)	0.605
Multiple lesions at baseline						
Single lesion	1		1		1	
Multiple lesions	2.2 (0.5-9.9)	0.323	2.86 (1.57-5.21)	0.001	1.93 (1.14-3.27)	0.014
Macroscopic portal vein thrombosis						
No	1		1		1	
Yes	11.1 (2.4-51.4)	0.002	1.73 (0.8-3.75)	0.166	1.75 (0.85-3.61)	0.127
Location near liver dome						
>1 cm away from dome	1		1		1	
≤1 cm away from dome	1.4 (0.24-7.78)	0.717	2.14 (1.15-3.97)	0.016	1.79 (1.01-3.18)	0.046
Location near liver capsule						
>1 cm away from capsule	1		1		1	
≤1 cm away from capsule	1.5 (0.3-7.9)	0.644	1.45 (0.78-2.9)	0.289	1.26 (0.68-2.3)	0.464
Location of tumour						
Right lobe	1		1		1	
Left lobe	2.1 (0.4-11.4)	0.369	1.45 (0.73-2.88)	0.286	1.03 (0.54-1.96)	0.929
Pattern of lipiodol stain (if any)						
Minimal	NA		1	0.024	1	0.138
Partial or heterogeneous	NA		0.27 (0.09-0.83)	0.022	0.49 (0.16-1.47)	0.203
Diffuse or homogeneous	NA		0.18 (0.54-0.62)	0.006	0.31 (0.1-1.03)	0.055
Presence of focal liver reaction in post-treatment computed tomography						
No	1		1		1	
Yes	0.49 (0.09-2.78)	0.422	0.67 (0.35-1.29)	0.234	0.4 (0.23-0.72)	0.002
Presence of focal liver reaction in post-treatment magnetic resonance imaging						
No	1		1		1	
Yes	0.17 (0.01-2.7)	0.210	0.37 (0.1-1.46)	0.157	0.28 (0.09-0.85)	0.026
T1-weighted signal intensity in post-treatment magnetic resonance imaging						
Hypointense	1		1		1	
Hyperintense	0.14 (0.01-2.2)	0.160	0.18 (0.04-0.84)	0.029	0.55 (0.15-1.97)	0.358
T2-weighted signal intensity in post-treatment magnetic resonance imaging						
Hypointense	NA		1		1	
Hyperintense	NA		9.54 (1.53-59.48)	0.016	8.99 (1.43-56.6)	0.019
Complete thin rim enhancement in post-treatment images						
No	1		1		1	
Yes	0.12 (0.01-1.1)	0.061	0.25 (0.12-0.51)	<0.001	0.33 (0.18-0.63)	0.001

Abbreviations: HR = hazard ratio; 95% CI = 95% confidence interval; mRECIST = modified Response Evaluation Criteria in Solid Tumors; NA = not applicable.

\* Data are shown as No. (%) or median (95% confidence interval).

was 20 months. Overall survival rate at 1 year and 2 years were 76% and 48%, respectively.

The results of the univariate Cox regression analyses are detailed in Table 5. For in-field local control, macroscopic portal vein thrombosis was shown to be significant predictive factor (HR: 11.1,  $p = 0.002$ ). For progression (in-field, out-of-field and extrahepatic metastasis), unfavourable factors included multiplicity of lesions

(HR: 2.86,  $p = 0.001$ ), location near liver dome (HR: 2.14,  $p = 0.016$ ) and T2-weighted hyperintense signal in post-treatment MRI (HR: 9.54,  $p = 0.016$ ). Favourable factors included pattern of lipiodol stain (partial stain HR: 0.27,  $p = 0.022$ ; diffuse stain HR: 0.18,  $p = 0.006$ ), T1-weighted hyperintense signal in post-treatment MRI (HR: 0.18,  $p = 0.029$ ) and complete thin rim enhancement in post-treatment images (HR: 0.25,  $p < 0.001$ ). For overall survival, unfavourable imaging factors included

multiplicity of lesions (HR: 1.93,  $p = 0.014$ ), location near liver dome (HR: 1.79,  $p = 0.046$ ) and T2-weighted hyperintense signal in post-treatment MRI (HR: 8.99,  $p = 0.019$ ). Favourable imaging predictors included focal liver reaction in post-treatment CT or MRI (HR: 0.4,  $p = 0.002$ ; HR: 0.28,  $p = 0.026$ ), and complete thin rim enhancement in post-treatment images (HR: 0.33,  $p = 0.001$ ).

In multivariable proportional hazards regression model, location near dome (HR = 5.8,  $p < 0.001$ ), pattern of lipiodol stain ( $p = 0.048$ ) and complete thin rim enhancement in post-treatment images (HR = 0.26,  $p = 0.003$ ) were shown to be significant predictors for progression. Complete thin rim enhancement (HR = 0.37,  $p = 0.002$ ) and focal liver reaction in post-treatment images (HR = 0.43,  $p = 0.009$ ) were shown to be significant predictors for overall survival (Table 6).

## DISCUSSION

Our results highlight the importance of post-treatment radiological changes as predictors for local control, disease progression, and overall survival.

The goal of radiotherapy is tumour cell death and necrosis. The central area of coagulative necrosis may be seen within the tumour. This coagulative necrosis will result in hyperdensity in CT or hyperintense signal on T1-weighted imaging, thus limiting assessment for residual tumour enhancement. Subtraction images can be a helpful adjunct for differentiating coagulative necrosis from enhancing tumour on MRI imaging. Hyperintense appearance on T2-weighted imaging with associated nodular enhancement is a characteristic of tumour or incompletely treated tumour.<sup>9</sup> Our results were in keeping with the fact that non-viable tumour (tumour T1-weighted hyperintense signal in post-treatment MRI) was associated with better prognosis and viable tumour

(tumour T2-weighted hyperintense signal in post-treatment MRI) was associated with worse prognosis (Figures 4 and 5).

Nearly half of the patients in our cohort had previous TACE before SBRT for HCC. An extensive amount of lipiodol deposited within the target lesion was also highly associated with the finding of >90% tumour necrosis.<sup>12</sup> Tumour portions that retained lipiodol were more likely to be necrotic at pathology. Conversely, lesions demonstrating incomplete staining with lipiodol and residual enhancement were more likely to contain viable tumour. This was also in keeping with our findings that patients with tumours showing diffuse lipiodol stain attained better prognosis (Figure 6). Lipiodol-stained lesion is also favourable in image guidance by improving the accuracy and precision for patient setup prior to SBRT. Up to 76% of the image guidance for HCC SBRT in our centre was lipiodol defined.<sup>22</sup>

Focal liver reaction over irradiated juxtaposed non-tumourous hepatic parenchyma can occur after SBRT. The extent and degree of focal liver reaction is multifactorial. The predominant histological changes are subtotal collagenous occlusion of small hepatic vein branches, hyperaemia, and diminished cellularity. The imaging appearances of the irradiated liver parenchyma likely reflect increased water content and impaired perfusion, with characteristic hypoattenuation on CT imaging, signal hypointensity on T1-weighted MR imaging, and signal hyperintensity on T2-weighted MR imaging. After SBRT, the shape of the treated zone may be complex and non-anatomical (not corresponding to a vascular territory or segment) because of the three-dimensional beam geometry.<sup>25</sup> Histological findings of veno-occlusive disease and imaging findings of hepatic changes are more persistently seen after 6 months, in which arterial phase hyperenhancement is due to

**Table 6.** Multivariable hazard model of radiological predictive factors for primary and secondary outcomes.

Radiological features	Time to progression		Overall survival	
	HR (95% CI)	p Value	HR (95% CI)	p Value
Location near liver dome				
≤1 cm vs. >1 cm away from dome	5.8 (2.3-14.9)	<0.001	NA	
Pattern of lipiodol stain (if any)		0.048	NA	
Partial or heterogeneous vs. minimal	0.21 (0.05-0.87)	0.032	NA	
Diffuse or homogeneous vs. minimal	0.16 (0.04-0.69)	0.014	NA	
Complete thin rim enhancement in post-treatment images (Yes vs. No)	0.26 (0.1-0.64)	0.003	0.37 (0.2-0.7)	0.002
Presence of focal liver reaction in post-treatment computed tomography (Yes vs. No)		NA	0.43 (0.23-0.81)	0.009



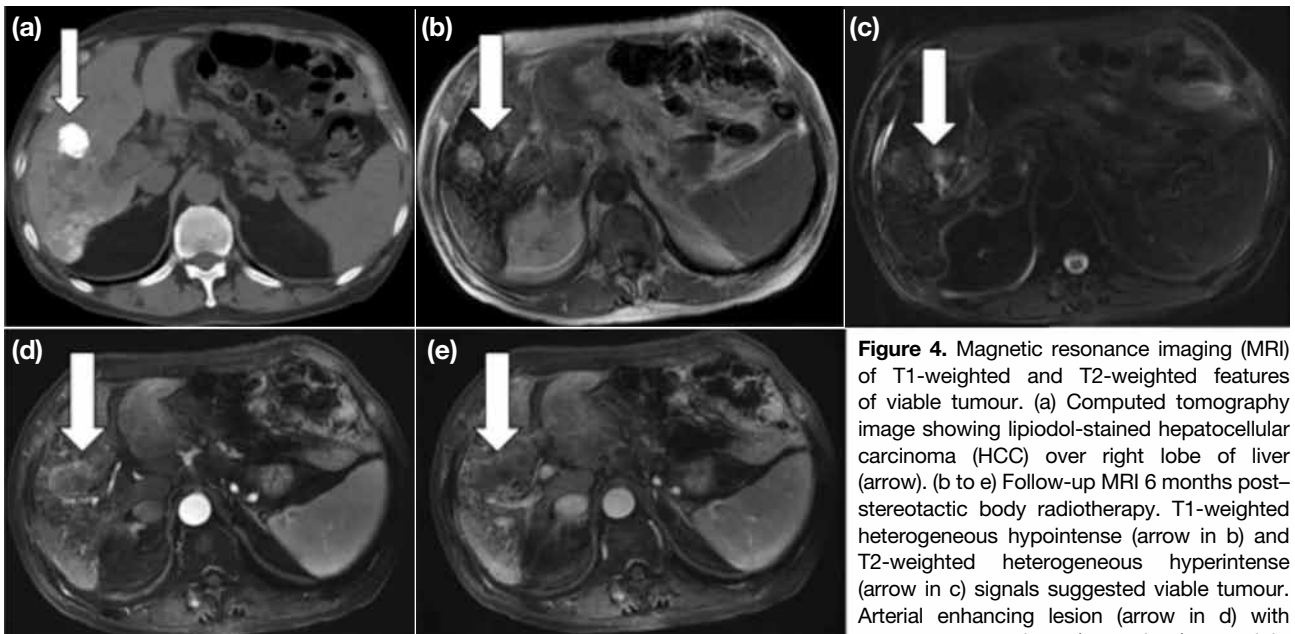


**Figure 4.** Magnetic resonance imaging (MRI) of T1-weighted and T2-weighted features of viable tumour. (a) Computed tomography image showing lipiodol-stained hepatocellular carcinoma (HCC) over right lobe of liver (arrow). (b to e) Follow-up MRI 6 months post-stereotactic body radiotherapy. T1-weighted heterogeneous hypointense (arrow in b) and T2-weighted heterogeneous hyperintense (arrow in c) signals suggested viable tumour. Arterial enhancing lesion (arrow in d) with portovenous washout (arrow in e) over right lobe liver confirmed viable HCC.

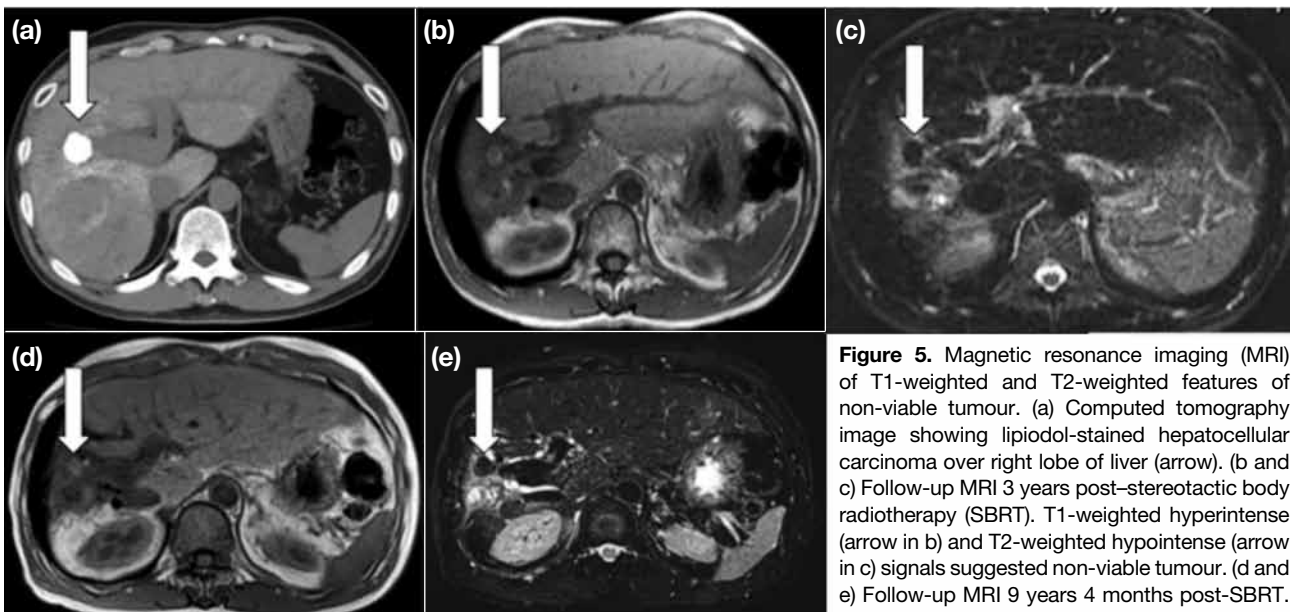


**Figure 5.** Magnetic resonance imaging (MRI) of T1-weighted and T2-weighted features of non-viable tumour. (a) Computed tomography image showing lipiodol-stained hepatocellular carcinoma over right lobe of liver (arrow). (b and c) Follow-up MRI 3 years post-stereotactic body radiotherapy (SBRT). T1-weighted hyperintense (arrow in b) and T2-weighted hypointense (arrow in c) signals suggested non-viable tumour. (d and e) Follow-up MRI 9 years 4 months post-SBRT. T1-weighted hyperintense (arrow in d) and T2-weighted hypointense (arrow in e) signals were similarly noted. No evidence of local tumour progression.

preserved arterial inflow into the focal liver reaction, which may remain hyperenhanced in the delay phase. This was thought to be due to fibrosis of the central veins, delay clearance, and stasis of contrast.<sup>17</sup> Presence of focal liver reaction was shown to have favourable prognosis in our cohort, probably due to vascular damage, in addition to the radiation tumouricidal ablative effect (Figure 7). Continuous thin rim of enhancement may be

seen in follow-up imaging. Care should be taken not to diagnose peripheral regrowth when a thin, regular rim of progressive enhancement is present because this finding is a sign of simple vascularised inflammation, focal liver reaction, or fibrosis.<sup>9</sup> It can be present during chronic (>6 months) phase and persists for years. Nodular rim, rim showing washout, or rim similar to tumour before treatment should raise the suspicion of residual or

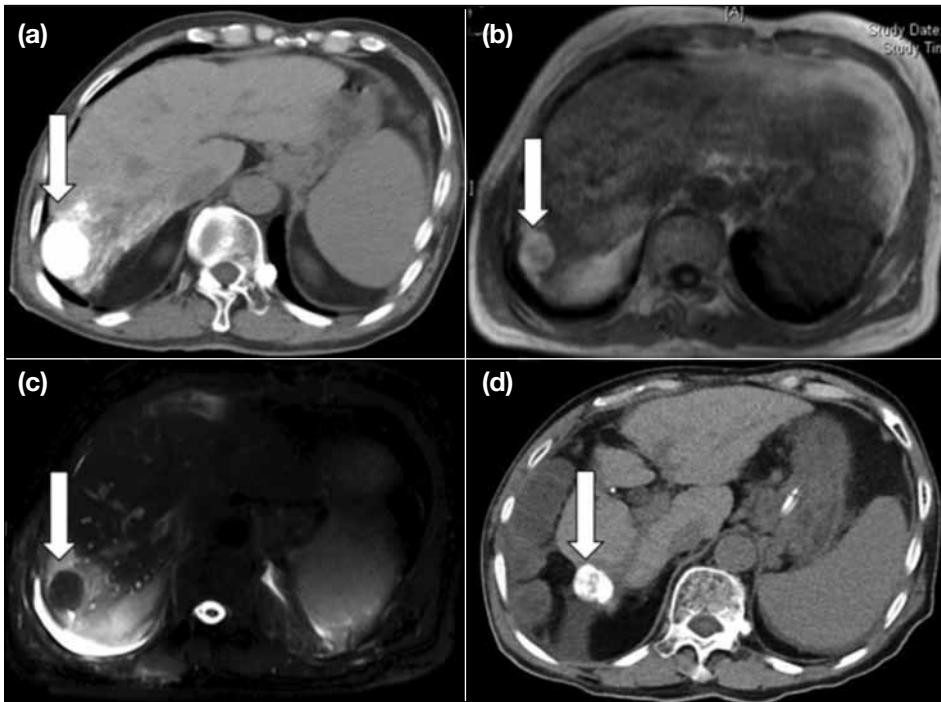


**Figure 6.** Lipiodol-stained pattern of hepatocellular carcinoma (HCC). (a) Computed tomography (CT) image showing diffuse lipiodol-stained HCC over right lobe of liver (arrow). (b and c) Follow-up magnetic resonance imaging 3 years post-stereotactic body radiotherapy (SBRT). T1-weighted hyperintense (arrow in b) and T2-weighted hypointense (arrow in c) signals suggested nonviable tumour. (d) Follow-up CT 5 years 2 months post-SBRT. No evidence of local tumour progression (arrow). The patient died of chest infection 6 years 3 months post-SBRT. Diffuse lipiodol-stained pattern carried better prognosis when compared with those with minimal or partial lipiodol-stained pattern.

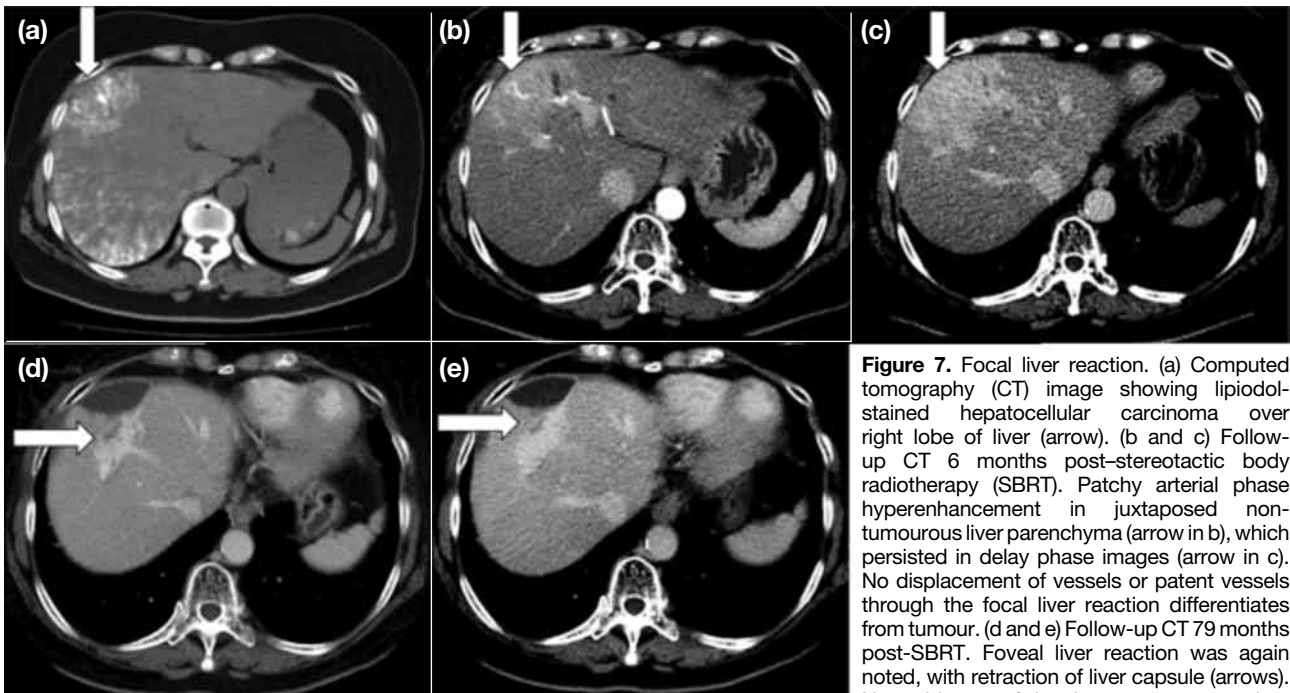


**Figure 7.** Focal liver reaction. (a) Computed tomography (CT) image showing lipiodol-stained hepatocellular carcinoma over right lobe of liver (arrow). (b and c) Follow-up CT 6 months post-stereotactic body radiotherapy (SBRT). Patchy arterial phase hyperenhancement in juxtaposed non-tumourous liver parenchyma (arrow in b), which persisted in delay phase images (arrow in c). No displacement of vessels or patent vessels through the focal liver reaction differentiates from tumour. (d and e) Follow-up CT 79 months post-SBRT. Foveal liver reaction was again noted, with retraction of liver capsule (arrows). No evidence of local tumour progression. Presence of focal liver reaction appears to have favourable prognosis, probably due to protective effect of vascular damage.

recurrent tumour. Continuous progressive or persistent thin rim enhancement in post-treatment images is a good radiological prognostic feature (Figure 8).

This study has several limitations. This was a retrospective study with inherent limitations. The number of patients receiving progress MRI was limited (n =

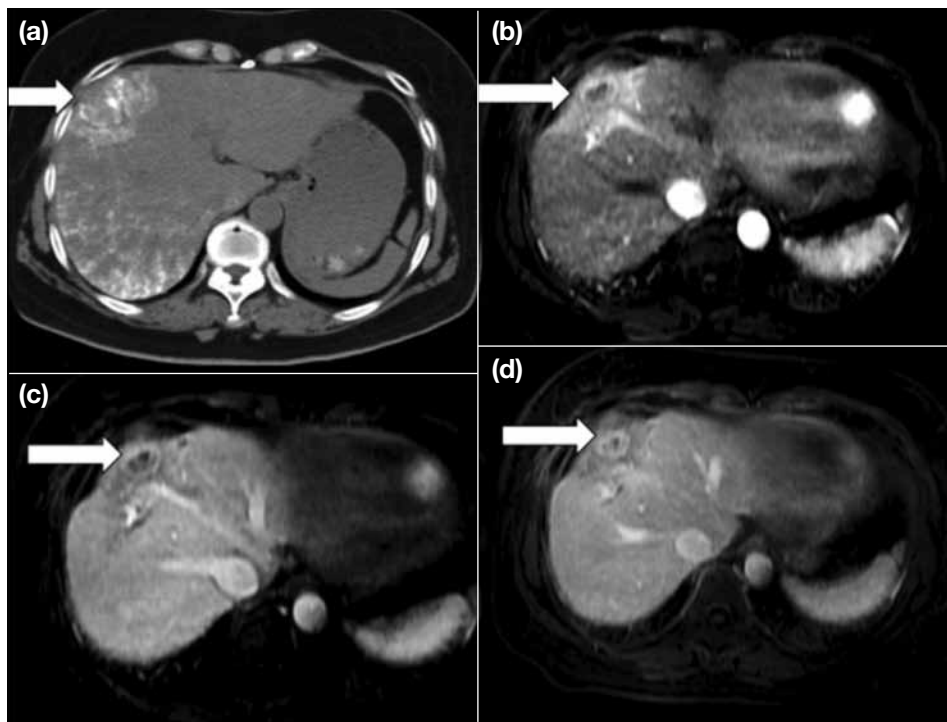


**Figure 8.** Continuous complete thin rim enhancement. (a) Computed tomography image showing lipiodol-stained hepatocellular carcinoma over right lobe of liver (arrow). (b to d) Follow-up magnetic resonance images 11 months post-stereotactic body radiotherapy (SBRT). There was continuous complete thin rim enhancement of the treated lesion, with persisted in arterial, portovenous and delay phase images (arrows in b to d). The patient survived 81 months post-SBRT. Continuous thin rim of enhancement probably represents focal liver reaction or inflammatory response and should not be interpreted as residual tumour. Nodular rim, rim showing washout or rim similar to tumour before treatment should raise the suspicion of residual or recurrent tumour.

26). Multivariable Cox regression uses complete case analysis, so if any of the predictors contain missing data, the whole case will be excluded from the regression. If MRI predictors were included into the regression model, then the number of cases used for regression would be  $\leq 26$ . Therefore, the MRI-only features variables had to be excluded from the multivariable model due to limited sample size, including potentially useful imaging parameters such as diffusion weighted imaging and apparent diffusion coefficient value. The study contains a very heterogeneous group of patients, whose baseline characteristics would confound the outcomes. For example, Barcelona Clinic Liver Cancer stage D patients may carry worse prognosis. It is difficult to control all confounding factors given the limited number of subjects. For example, superselective or ultraslective TACE with good lipiodol uptake is potentially curative. The effect of SBRT cannot be exactly determined in this group of patients. Nine patients in our cohort received SBRT without any prior treatment. Whether their outcomes differ significantly when compared with those receiving prior therapies is not well studied. A prospective study with a larger study population may be able to address these issues.

In keeping with previously published data,<sup>4,6,7,14,15,26</sup> the

local control rate in our cohort was high, with reasonable overall survival. These results are promising for these patients; in addition to their HCC being inoperable, further TACE treatment was not feasible due to TACE complications or unsatisfactory response with previous TACE treatment. SBRT is a feasible treatment option for patients with locally advanced or unresectable HCC.

## CONCLUSION

Imaging evaluation of tumour response is important. Recognising and interpreting the radiological features of tumour response is essential in making an accurate assessment and guide subsequent disease management. Accurate imaging evaluation may also help predict survival.

## REFERENCES

1. Parkin DM, Bray F, Ferlay J, Pisani F. Global cancer statistics, 2002. *CA Cancer J Clin.* 2005;55:74-108. [Crossref](#)
2. Hong Kong Cancer Registry, Hospital Authority. Hong Kong Cancer Statistics 2016. Available from: <http://www3.ha.org.hk/cancereg/pdf/overview/Summary%20of%20CanStat%202016.pdf>. Accessed 14 Aug 2019.
3. European Association for the Study of the Liver. EASL Clinical Practice Guidelines: Management of hepatocellular carcinoma. *J Hepatol.* 2018;69:182-236. [Crossref](#)
4. Su TS, Liang P, Lu HZ, Liang J, Gao YC, Zhou Y, et al. Stereotactic body radiation therapy for small primary or recurrent

- hepatocellular carcinoma in 132 Chinese patients. *J Surg Oncol.* 2016;113:181-7. [Crossref](#)
5. Scorsetti M, Comito T, Cozzi L, Clerici E, Tozzi A, Franzese C, et al. The challenge of inoperable hepatocellular carcinoma (HCC): Results of a single-institutional experience on stereotactic body radiation therapy (SBRT). *J Cancer Res Clin Oncol.* 2015;141:1301-9. [Crossref](#)
  6. Sanuki N, Takeda A, Oku Y, Mizuno T, Aoki Y, Eriguchi T, et al. Stereotactic body radiotherapy for small hepatocellular carcinoma: A retrospective outcome analysis in 185 patients. *Acta Oncol.* 2014;53:399-404. [Crossref](#)
  7. Kang JK, Kim MS, Cho CK, Yang KM, Yoo HJ, Kim JH, et al. Stereotactic body radiation therapy for inoperable hepatocellular carcinoma as a local salvage treatment after incomplete transarterial chemoembolization. *Cancer.* 2012;118:5424-31. [Crossref](#)
  8. Yaghmai V, Besa C, Kim E, Gatlin JL, Siddiqui NA, Taouli B. Imaging assessment of hepatocellular carcinoma response to locoregional and systemic therapy. *AJR Am J Roentgenol.* 2013;201:80-96. [Crossref](#)
  9. Sanuki N, Takeda A, Mizuno T, Oku Y, Eriguchi T, Iwabuchi S, et al. Tumor response on CT following hypofractionated stereotactic ablative body radiotherapy for small hypervascular hepatocellular carcinoma with cirrhosis. *AJR Am J Roentgenol.* 2013;201:W812-20. [Crossref](#)
  10. Shim JH, Lee HC, Kim SO, Shin YM, Kim KM, Lim YS, et al. Which response criteria best help predict survival of patients with hepatocellular carcinoma following chemoembolization? A validation study of old and new models. *Radiology.* 2012;262:708-18. [Crossref](#)
  11. Sanuki-Fujimoto N, Takeda A, Ohashi T, Kunieda E, Iwabuchi S, Takatsuka K, et al. CT evaluations of focal liver reactions following stereotactic body radiotherapy for small hepatocellular carcinoma with cirrhosis: Relationship between imaging appearance and baseline liver function. *Br J Radiol.* 2010;83:1063-71. [Crossref](#)
  12. Kwan SW, Fidelman N, Ma E, Kerlan RK Jr, Yao FY. Imaging predictors of the response to transarterial chemoembolization in patients with hepatocellular carcinoma: A radiological-pathological correlation. *Liver Transpl.* 2012;18:727-36. [Crossref](#)
  13. An C, Kim DW, Park YN, Chung YE, Rhee H, Kim MJ. Single hepatocellular carcinoma: Preoperative MR imaging to predict early recurrence after curative resection. *Radiology.* 2015;276:433-43. [Crossref](#)
  14. Bibault JE, Dewas S, Vautravers-Dewas C, Hollebecque A, Jarraya H, Lacomere T, et al. Stereotactic body radiation therapy for hepatocellular carcinoma: Prognostic factors of local control, overall survival, and toxicity. *PLoS One.* 2013;8:e77472. [Crossref](#)
  15. Lo CH, Yang JF, Liu MY, Jen YM, Lin CS, Chao HL, et al. Survival and prognostic factors for patients with advanced hepatocellular carcinoma after stereotactic ablative radiotherapy. *PLoS One.* 2017;12:e0177793. [Crossref](#)
  16. Oldrini G, Huertas A, Renard-Oldrini S, Taste-George H, Vogin G, Laurent V, et al. Tumor response assessment by MRI following stereotactic body radiation therapy for hepatocellular carcinoma. *PLoS One.* 2017;12:e0176118. [Crossref](#)
  17. Haddad MM, Merrell K, Johnson GB, Hallemeier CL, Olivier KR, Fidler JF, et al. Stereotactic body radiation therapy (SBRT) of liver tumors: Imaging appearances and implications on evaluation of response. *Radiology and Radiation Oncology*, Mayo Clinic, Rochester, Minnesota; 2017.
  18. Miller AB, Hoogstraten B, Staquet M, Winkler A. Reporting results of cancer treatment. *Cancer.* 1981;47:207-14. [Crossref](#)
  19. Therasse P, Arbuck SG, Eisenhauer EA, Wanders J, Kaplan RS, Rubinstein L, et al. New guidelines to evaluate the response to treatment in solid tumors. European Organization for Research and Treatment of Cancer, National Cancer Institute of the United States, National Cancer Institute of Canada. *J Natl Cancer Inst.* 2000;92:205-16. [Crossref](#)
  20. Bruix J, Sherman M, Llovet JM, Beaugrand M, Lencioni R, Burroughs AK, et al. Clinical management of hepatocellular carcinoma. Conclusions of the Barcelona-2000 EASL conference. European Association for the Study of the Liver. *J Hepatol.* 2001;35:421-30. [Crossref](#)
  21. Lencioni R, Llovet JM. Modified RECIST (mRECIST) assessment for hepatocellular carcinoma. *Semin Liver Dis.* 2010;30:52-60. [Crossref](#)
  22. Law AL, Ng WT, Lee MC, Chan AT, Fung KH, Li F, et al. Treatment of primary liver cancer using highly-conformal radiotherapy with kV-image guidance and respiratory control. *Radiother Oncol.* 2012;102:56-61. [Crossref](#)
  23. Radiation Therapy Oncology Group. Randomized phase III study of sorafenib versus stereotactic body radiation therapy followed by sorafenib in hepatocellular carcinoma. RTOG 1112, version date Nov 30, 2012. Available from: [https://www.rtog.org/Portals/0/RTOG Broadcasts/Attachments/1112\\_master\\_w\\_update\\_5.7.13.pdf](https://www.rtog.org/Portals/0/RTOG%20Broadcasts/Attachments/1112_master_w_update_5.7.13.pdf). Accessed 28 Aug 2019.
  24. Maturen KE, Feng MU, Wasnik AP, Azar SF, Appelman HD, Francis IR, et al. Imaging effects of radiation therapy in the abdomen and pelvis: Evaluating “innocent bystander” tissues. *Radiographics.* 2013;33:599-619. [Crossref](#)
  25. Lee MT, Kim JJ, Dinniwell R, Brierley J, Lockwood G, Wong R, et al. Phase I study of individualized stereotactic body radiotherapy of liver metastases. *J Clin Oncol.* 2009;27:1585-91. [Crossref](#)
  26. Lam MH, Cheng HC, Ngan RK. Stereotactic body radiation therapy for hepatocellular carcinoma: Review of a local hospital. *Hong Kong J Radiol.* 2017;20:205-12. [Crossref](#)